UNCERTAINTIES IN THE INVERSE MODELLING OF SULPHUR DIOXIDE ERUPTION PROFILES

Petra Seibert[1], Sabine Eckhardt[2], Nina Kristiansen[2], Fred Prata[2], Andreas Richter[3], Andreas Stohl[2]

[1]Institute of Meteorology (BOKU-Met), University of Natural Resources and Applied Life Sciences Vienna (BOKU), Austria

petra.seibert@boku.ac.at, http://met.boku.ac.at/

[2] NILU, Norway http://met.boku.ac.at/ [3] University of Bremen, Institute for Environmental Physics, Germany http://www.iup.uni-bremen.de/

Introduction

We have developed a methodology for retrieving vertical profiles of the source term in volcanic eruption columns, based on satellite column data obtained during the following hours and days on one hand and transport and dispersion calculations with FLEXPART on the other. These two pieces of information are used as input for an analytical inversion algorithm. So far, the method was applied for sulphur dioxide emissions at Jebel at Tair (Eckhardt et al., 2008) and Kasatochi (Kristiansen et al., 2010). GOME, OMI, SEVIRI, and AIRS data have been used in different combinations. The inversion uses as input an a priori profile together with its uncertainty, usually a very simple shape, and the column values from the satellite retrieval, also with uncertainties. The uncertainties are only rough estimates. The impact of assuming different a priori assumptions on the final profiles and their a posteriori uncertainty is studied. The a posteriori uncertainty of the retrieved emission profile is a new feature in our algorithm presented here for the first time.

The Kasatochi 2008 eruption

Figure 1: The volcanic island of Kasatochi before and after the VEI 4 eruption in August 2008 (photographs from Alaska Volcano Observatory (AVO), http://www.avo.alaska.edu/.

Kasatochi Volcano is a small unpopulated island (Fig. 1) on the Aleutian arc. The active stratovolcano reaches only 314 m a.s.l. and lay dormant for 200 years.

The eruption in August 2008

- Three eruptions: 2008-08-07 22:01 UTC, 2009-08-08 01:50 UTC and 04:35 UTC
- Eruptions reached the stratosphere, to a top exceeding 15 km while the tropopause was at about 10 km.
- All eruptions emitted SO_2, about 1.2 ? 2.5 Tg, the largest SO_2 mass loadings since the Cerro Hudson 1991 in Chile
- The third eruption was accompanied and followed by massive ash emission, Alaska Airlines was forced to cancel 44 flights between 10 and 11 August 2008
- The ash travelled along with the SO_2 for about 3 d, thus SO_2 may also serve as a proxy for ash

Inverse modelling of the volcanic emission

In Kristiansen et al. (2010), inverse modelling of the the SO_2 emission from Kasatochi has been performed with the methodology introduced in Eckhardt et al. (2008). The method has three major components:

1. SO_2 column values derived from different satellites
2. Forward dispersion modelling with the Lagrangian particle model FLEXPART (Stohl et al. 2005)
3. Inversion procedure based on the components 1 and 2 (Seibert 1999, Eckhardt et al. 2008)

FLEXPART simulations with the derived source term have been compared with satellite observations at later dates and laser observations (CALIPSO and surface-based lidar), showing that the method works well.

Acknowledgement

This work is carried out in the context of the project *Support to Aviation for Volcanic Ash Avoidance* (SAVAA, http://savaa.nilu.no/), financed in the European Space Agency's *Earth Observation Envelope Programme* (EOEP) – Data User Element.

This poster has been produced with free software (LaTeX with beamerposter).

Inverse modelling of the volcanic emission (cont.)

Compared to the Kristiansen et al. (2010) paper, this poster

- uses only GOME-2 data as input, from four overpasses, of which two captured the whole plume (Fig. 2)
- systematically studies variations in adjustable input parameters (a priori emission profile, a priori uncertainties of both the first-guess emission profile and the satellite data)
- presents a posteriori uncertainties of the reconstructed emission profile.

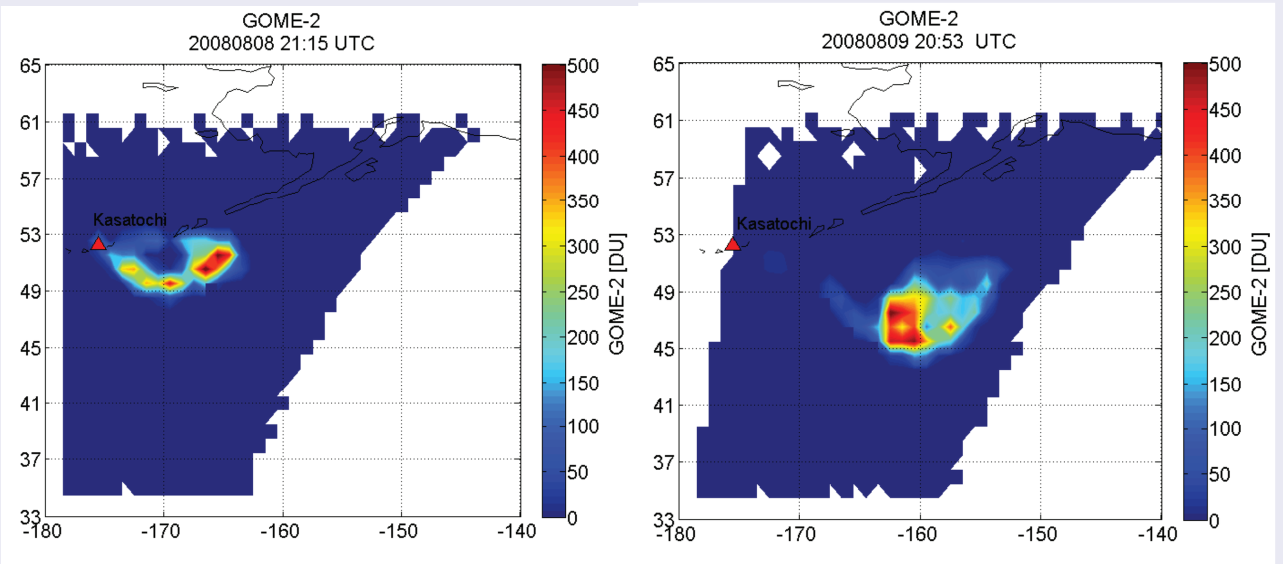

Figure 2: SO_2 column values retrieved from GOME-2 for the two main overpasses. Kasatochi is marked by a red triangle.

Inversion procedure

- Modelled column values $\mathbf{y} = \mathbf{M}\mathbf{x}$
  where $\mathbf{x}$ is the vector of $x_1, \ldots, x_n$ source contributions and
  $\mathbf{M}$ is the $m \times n$ source-receptor matrix (m is the number of observed values)
- Observed values $\mathbf{y^o}$
- Cost function $J = J_1 + J_2 + J_3$ with

$$\begin{aligned} J_1 &= (\mathbf{Mx}-\mathbf{y})^T \mathbf{diag}(\boldsymbol{\sigma}_\mathbf{o}{}^{-2})\,(\mathbf{Mx}-\mathbf{y}) && \text{misfit model–observation}\\ J_2 &= \mathbf{x}^T\mathbf{diag}(\boldsymbol{\sigma}_\mathbf{x}{}^{-2})\,\mathbf{x} && \text{deviation from a priori}\\ J_3 &= \epsilon\,(\mathbf{Dx})^T\mathbf{Dx} && \text{deviation from smoothness}\end{aligned}$$

- Minimisation of J leads to linear system of equations of size n, solves very quickly
- Ensuring solution with only positive values by placing penalties on negative values (increasing $\boldsymbol{\sigma}_\mathbf{x}{}^{-2}$) and iteration
- Additional inputs needed:
  - observation weights $\boldsymbol{\sigma}_o$ (were assumed as 20% of the observed value, but including a minimum value to ensure reasonable uncertainty on near-zero observations)
  - a priori values $\mathbf{x}^a$ and
  - their uncertainties $\boldsymbol{\sigma}_x$
  - value of smoothness parameter ϵ (empirical value)
- The a posteriori source profile $\tilde{\mathbf{x}}$ is obtained as

$$\mathbf{G}\tilde{\mathbf{x}} = \left(\mathbf{M}^T\,\mathbf{diag}(\sigma_\mathbf{o}{}^{-2})\mathbf{M} + \mathbf{diag}(\sigma_\mathbf{x}{}^{-2}) + \epsilon\,\mathbf{D}^T\mathbf{D}\right)\;\tilde{\mathbf{x}} = \sigma_o^{-2}\,\mathbf{M}^T\tilde{\mathbf{y}}$$

  where $\tilde{\mathbf{x}}, \tilde{\mathbf{y}}$ denote values with first guess subtracted.
- The a posteriori uncertainties are obtained as $\sigma_\mathbf{x}^\mathbf{b} = [\mathbf{diag}(\mathbf{G})]^{-1/2}$

References

Eckhardt S., A. J. Prata, P. Seibert, K. Stebel, and A. Stohl (2008) Estimation of the vertical profile of sulfur dioxide injection into the atmosphere by a volcanic eruption using satellite column measurements and inverse transport modeling. *Atmos. Chem. Phys.*,, http://www.atmos-chem-phys.net/8/3881/2008/

Kristiansen N. I., A. Stohl, A. J. Prata, A. Richter, S. Eckhardt, P. Seibert et al. (2010) Remote sensing and inverse transport modeling of the Kasatochi eruption sulfur dioxide cloud, to appear soon in *Journal of Geophysical Research*.

Seibert, P. (1999) Inverse Modelling of Sulfur Emissions in Europe Based on Trajectories. In: P. Kasibhatla et al. (editors), Inverse Methods in Global Biogeochemical Cycles, *AGU Geophysical Monograph Series*, Vol. 114, p. 147-154

Stohl, A., Forster, C., Frank, A., Seibert, P., and Wotawa, G. (2005) Technical note: The Lagrangian particle dispersion model FLEXPART version 6.2, *Atmos. Chem. Phys.*, http://www.atmos-chem-phys.net/5/2461

Parameter variation experiments

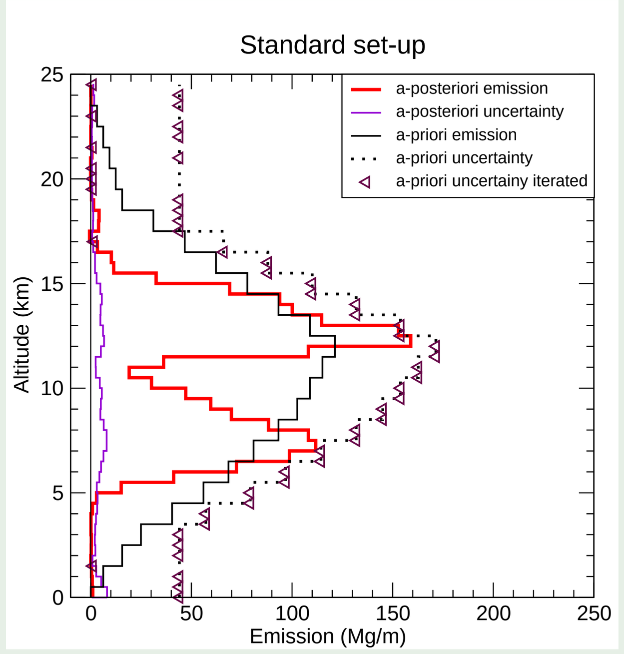

Figure 3: The standard set-up assumes a smooth a priori distribution with a maximum just above the tropopause. A priori uncertainties follow the a priori profile but retain a minimum of 45 Mg/m. 35% of mass.

A bimodal profile with a tropospheric peak at 7 km and a stratospheric peak at 12 km is obtained. Zero emissions result below 4 km and above 16 km. The uncertainties are greatly reduced and are on the order of only a few Mg/m. Increased regularisation in the iteration process to remove negative values occurs mainly in the upper part of the profile with near-zero values.

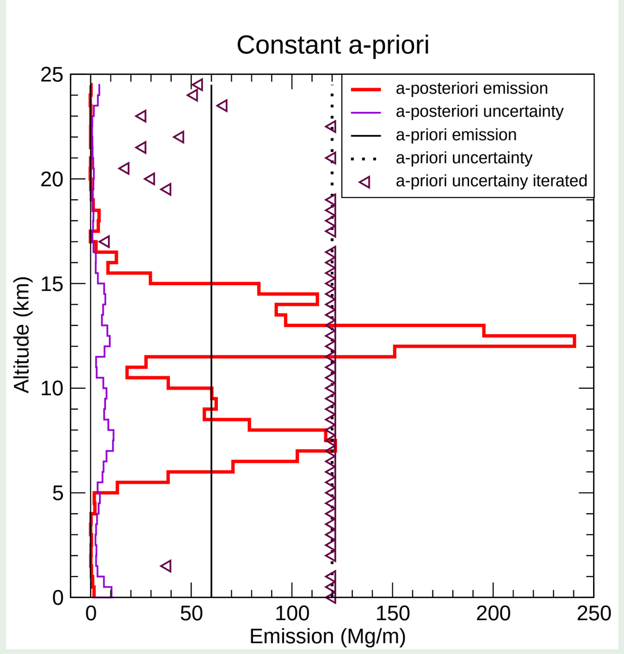

Figure 4: Constant a priori profile with 60 Mg/m and 120 Mg/m as uncertainty. This is also the base for all the following experiments. 40% of mass.

The height of the maxima and the region with zero emissions is identical to the standard set-up. The stratospheric peak becomes sharper and stronger. Both peaks show more structures but comparison with a posteriori uncertainties indicates that these structures are just noise.

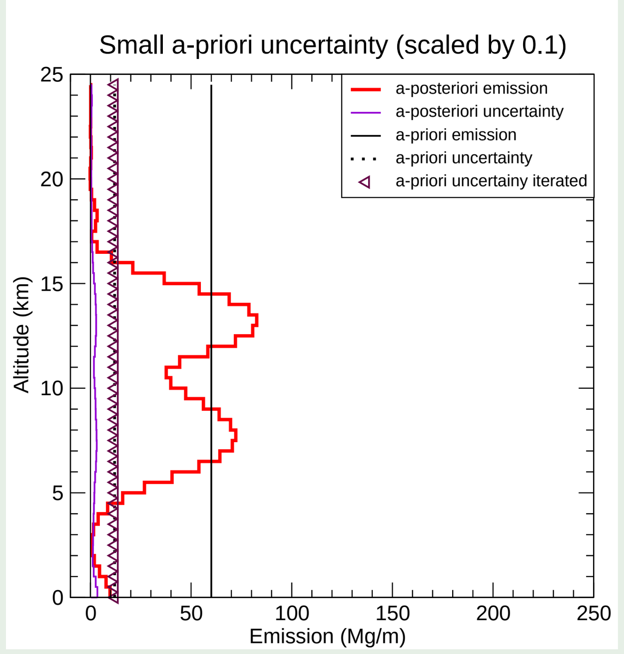

Figure 5: Same as Figure 4, but a priori uncertainties reduced from 120 to 12 Mg/m. 25% of mass.

As expected, everything becomes very smooth. A spurious maximum near the surface is introduced. The peak emissions are much reduced and the stratospheric peak is only marginally larger than the tropospheric one, but the height of the maxima remains the same.

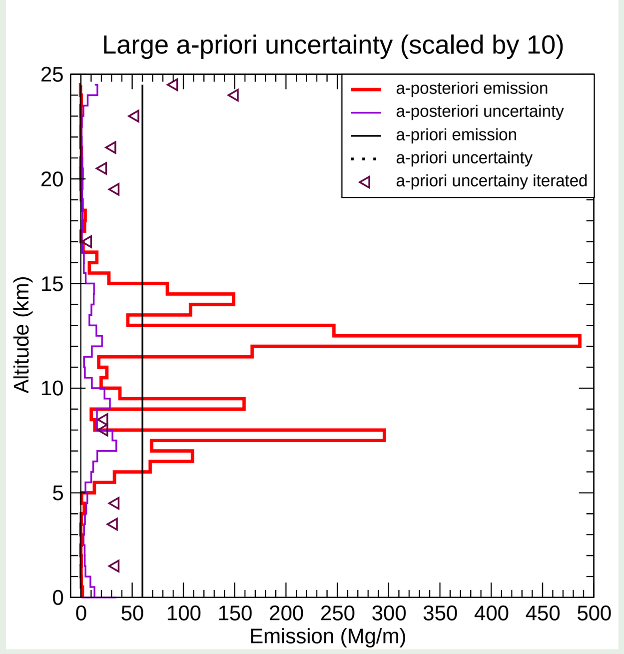

Figure 6: Same as Figure 4, but a priori uncertainties increased from 120 to 1200 Mg/m, thus outside the (enlarged!) scale. 49% of mass.

As expected, everything becomes more noisy. Regularisation to avoid negative values is invoked at more levels, including between the two peaks. The height of the peaks still is unchanged. The stratospheric maximum is very sharp and almost reaches 500 Mg/m!

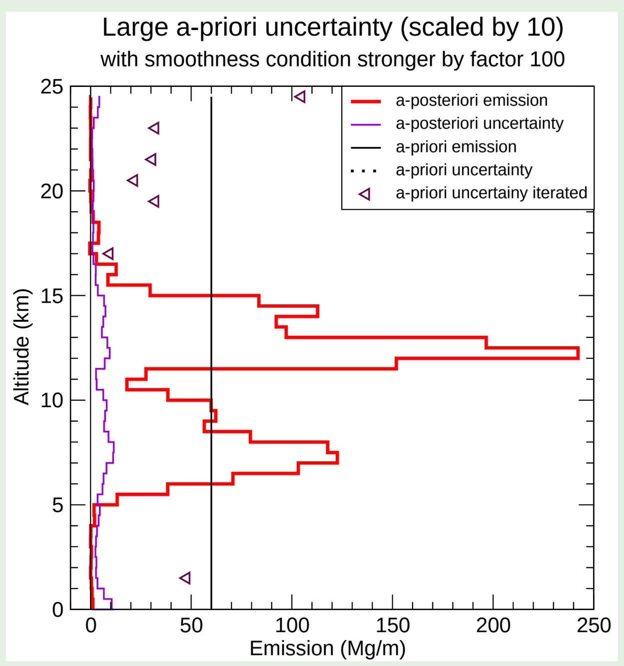

Figure 7: Same as Figure 6, but smoothness parameter ϵ is increased by a factor of 100 to counteract the noise. 40% of mass.

The results are almost identical with Figure 4, indicating that smoothness condition and a priority uncertainty can have very similar effects.

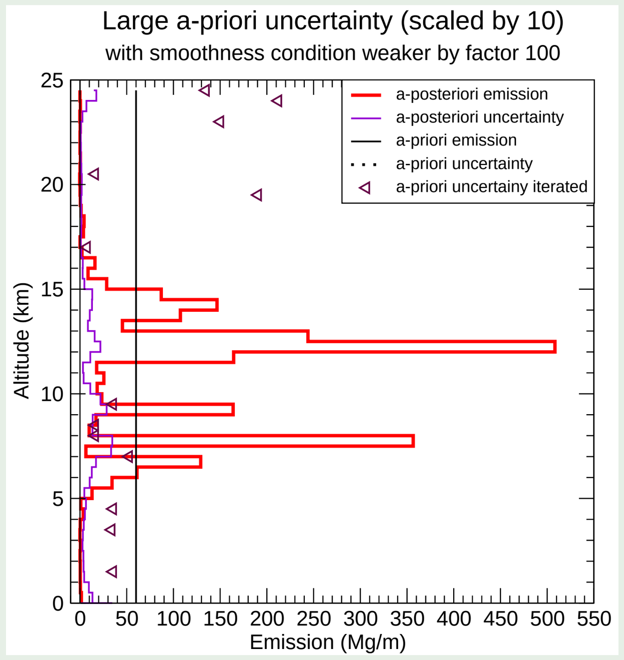

Figure 8: Same as Figure 6, but smoothness parameter ϵ is decreased by a factor of 100. 50% of mass.

The result is very similar to Figure 6, indicating that the value of the smoothness parameter applied there already has only little effect. A posteriori uncertainties go up to 40 Mg/m.

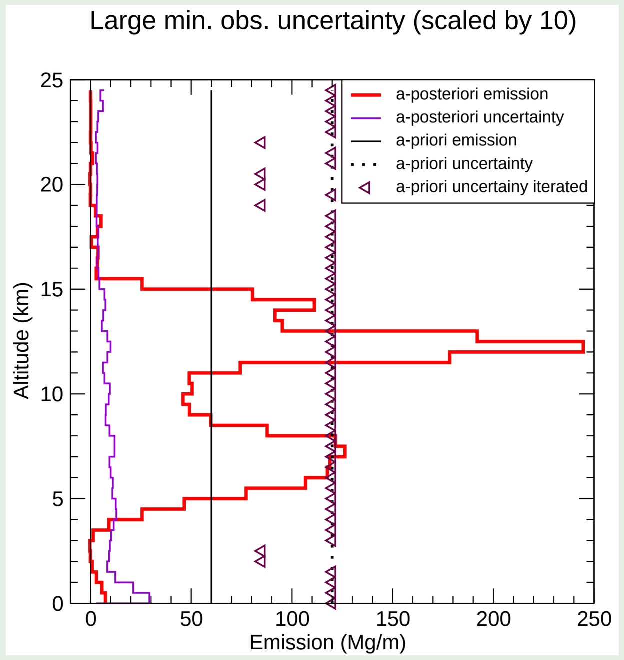

Figure 9: As in Figure 4, but minimum uncertainty for observations increased from 2 DU to 20 DU. 44% of mass.

A bit more of mass is recovered, mainly through a broader tropospheric peak. Some spurious emission close to the ground is produced.

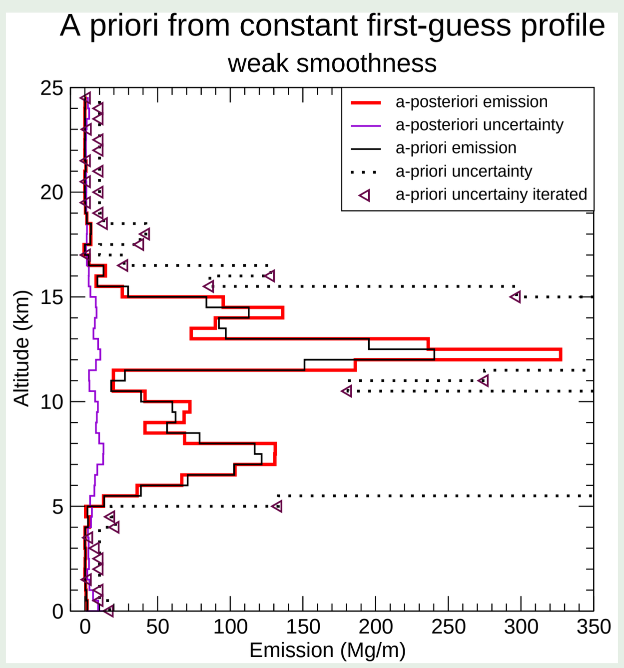

Figure 10: A priori profile taken from the result of the retrieval with simple assumptions (Figure 4) uncertainties assumed to be a factor of 10 of those values, with a minimum of 20 Mg/m, smoothness parameter reduced by factor of 100. 44% of mass.

This retrieval is only weakly regularised but uses a very good first-guess. The main difference is a sharper main peak. Additional regularisation for removing negative values is invoked only in the upper part of the profile, while the spurious emission close to the surface present in the first guess disappear.

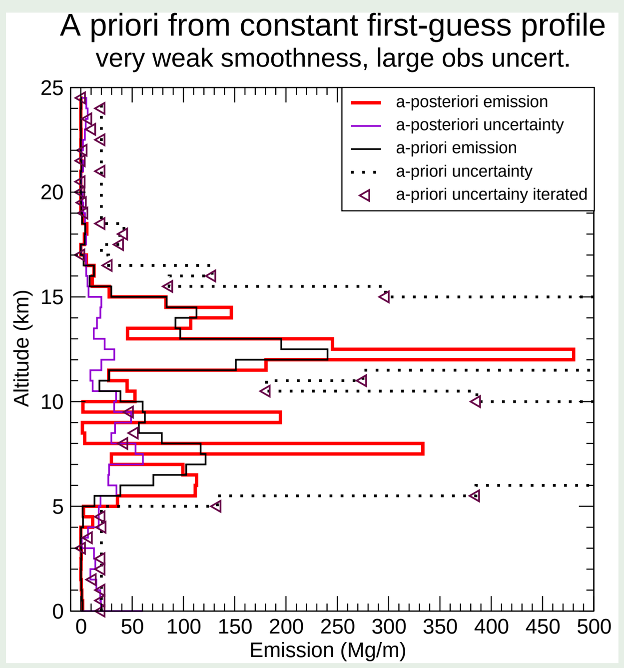

Figure 11: Same as Figure 10, but observation uncertainties increased by 50% compared to standard, 20 instead of 10 Mg/m minimun first guess uncertainty, and smoothness parameter reduced by a further factor 100, meaning that this condition is totally removed. 51% of mass.

Again, the stratospheric part of the profile is little changed, except that now the main peak is even more concentrated to the single layer of 12.0–12.5 km. The secondary maximum at 14 km is also more pronounced but is hardly significant if compared against the a posteriori sigma values. The tropospheric part is becoming considerably more noisy and uncertain.

Conclusions

1. The basic structure—a stratospheric and a tropospheric emission peak—and the heights of the peaks are extremely robust against all the parameter variations. Also the regions devoid of emissions are robust. All this is promising, although one has to be aware that this depends on the vertical wind profile and thus cannot be generalised.
2. Whenever the regularisation is weakened, the stratospheric peak becomes larger and sharper. This is probably realistic, and should be taken into account for further refinement of the standard set-up.
3. In all set-ups, only between 30% and 50% of the mass detected by the satellite is retrieved in the inversion. At the moment we can only speculate about the reasons. Ideas include
   - Contribution of the later eruptions (first tests seemed to indicate that they are difficult to separate through inversion, but this needs to be more carefully evaluated)
   - Weak constraint of the tropospheric part through the satellite data, might be larger (cf. Figure 9)
   - Errors in the transport simulation would lead to partly misaligned SO_2 cloud patterns, parts outside the observed cloud would be heavily penalised. A larger observation uncertainty as in Figure 9 counteracts this. Better quantification of transport uncertainty should then be helpful.
4. Within the SAVAA project, our method is being extended for volcanic ash and as we have seen in the Eyjafjallajökull eruption, a better definition of the source term could be very important for efficient support of VAAC operations. Including the temporal dimension of an eruption obviously is another task for the future.